https://doi.org/10.5194/os-2019-55
Preprint. Discussion started: 5 August 2019

Ocean Science Discussions
Open Access

Environmental controls on marine productivity near Cape St Francis, South Africa

Mark R Jury
University of Zululand, KwaDlangezwa, 3886, South Africa
and Physics Dept. Univ. of Puerto Rico, Mayaguez, USA, 00681

Abstract

This study considers ocean-atmosphere influences on marine productivity over the shelf near Cape St Francis, South Africa. Multi-day estimates of chlorophyll fluorescence in the period 2006-2017 with an area: 34.5-33.75S, 24-26.5E, provide the basis for evaluation using data from high resolution reanalysis.

Correlations with the mean annual cycle of chlorophyll fluorescence were significant for salinity, linking marine productivity and the coastal hydrology. A strengthened Agulhas Current induces cyclonic shear that lifts water at the shelf edge. Composite high chlorophyll fluorescence events were dominated by a large-scale mid-latitude atmospheric ridge of high pressure. The resultant easterly winds caused offshore transport and the upwelling of cool nutrient-rich water, in multi-day events at the beginning and end of austral summer. Environmental controls on inter-annual fluctuations of the commercial fishery were also explored. Southwestward currents and diminished heat fluxes favoured squid catch, while anchovy and sardine were linked with upper northerly wind, consistent with large-scale weather patterns that underpin coastal upwelling and river discharge. Productivity lags a few days behind cyclonic wind and current shear and the upstream coastal hydrology, which shares a common atmospheric driver.

mark.jury@upr.edu

1. Introduction

The southern coast of South Africa is swept by the prevailing warm Agulhas Current (Lutjeharms et al. 2000). Shelf-edge upwelling is induced by cyclonic shear of the current and downstream widening of the shelf (Schumann 1986, 1988, Lutjeharms 2006, Goschen et al. 2015, Malan et al. 2018). Coastal winds average 7 m/s (Schumann and Martin 1991) and tend to blow from east in summer and from west in winter. The easterlies lift cold nutrient-rich water next to three Capes: Padrone, Recife, St Francis, separating two sheltered bays (Schumann et al. 1982, Goschen and Schumann 1987, Schumann 1999, Schumann et al. 2005, Roberts 2010, Goschen and Schumann 2011, Pattrick et al. 2013). Rivers of the Eastern Cape discharge fresh silty water up to 100 m^3/s, during infrequent floods in the Gamtoos, Sundays and Fish River Valleys (Bladeren et al. 2007). Their plumes spread along the shore and into the large bays (Scharler and Baird 2005) and promote stratification in summer. Intra-seasonal fluctuations are attributed to pulsing and meandering of the Agulhas Current (Lutjeharms et al. 1989, Lutjeharms and Roberts 1988, Goschen and Schumann 1990, Rouault and Penven 2011) and by coastal low pressure cells coupled to shelf waves that pass eastward around South Africa, bringing changes in marine weather (Jury et al. 1990, Schumann and Brink 1990). Air-sea interactions exhibit cross-shore gradients that are important for coastal resources (Beckley 1988). The inshore bays are sheltered and develop stable layers during summer that aggregate phytoplankton. In this area known as the eastern Agulhas Bank, a commercial fishery aimed at sardines (67 K T/yr), squid (3K T/yr), anchovy, roman, mackerel, etc (Roberts et al. 2012, Cochrane et al. 2014) sees most catch effort within 50 km of the coast surrounding St Francis Bay (34S, 25E), which offers protection from persistent SSW swells (avg 2.3 m).

This study considers marine productivity at multi-day time-scales off Cape St Francis, South Africa. Using high resolution model-assimilated observations, our analysis seeks to understand how environmental conditions modulate chlorophyll and salinity. Section 2 covers the data and methods, while Section 3 presents the results progressing from mean features and statistics to case studies of productive events. Context is provided by temporal cross-correlations, spatial point-to-field regression and statistical comparison of commercial fish catch with environmental variables. Section 4 provides a discussion that relates the bio-chemistry indices to ocean-atmosphere forcing.

https://doi.org/10.5194/os-2019-55
Preprint. Discussion started: 5 August 2019

Ocean Science
Discussions

2. Data and Methods

A study is delimited to the productive eastern Agulhas Bank in the period of high resolution satellite coverage. Ocean conditions off Cape St Francis, South Africa (32.5–35S, 22–28.5E, Fig 1a) were described using multi-day SODA3 (25 km horizontal resolution, Carton et al. 2018) and daily HYCOM (GOFS3.1) reanalysis (9 km, Chassignet et al. 2009). These reanalysis (cf. Appendix) assimilate insitu observations from ship, buoy and drifter, and satellite infrared and microwave radiometer measurements over a multi-day period to produce a hindcast with a vertical resolution of < 5 m near the surface. Local validations are reported in Jury and Goschen (2019). Sea surface temperature (SST) was assimilated via daily 1 km infrared and 9 km microwave data after de-clouding and calibration (Chin et al. 2017). Salinity was assimilated via wide-swath passive microwave radiometers, while multiple zenith-pointing radar altimeters determined sea surface height and near-surface currents. Chlorophyll was estimated from MODIS satellite 4 km resolution green-band data, atmospheric corrected using an 8-day composite maximum and adjusted for radiometer drift (Hu et al. 2012). Similarly, the fluorescence line height was estimated from level-3 MODIS red-band data, which is less sensitive to coastal sediments (Gower 2016, Houskeeper and Kudela 2017). Swell characteristics were derived from the Wave-watch v3 hindcast (Tolman 2002). Atmospheric conditions were described using daily MERRA v2 reanalysis (50 km resolution, Gelaro et al. 2017). Winds were assimilated from station, ship and buoy measurements, blended with satellite cloud drift and active microwave scatterometer retrievals. The ocean reanalyses are embedded within the coupled data assimilation system: HYCOM from NCODA (Cummings and Smedstad 2013), and SODA3 from MERRA2 that incorporates hydrology and air chemistry (Reichle et al. 2017).

Daily and 8-day temporal records were extracted for an index-area 33.75–34.5S, 24–26.5E encompassing the shelf around Cape St Francis, South Africa (cf. Fig 1a). With two large bays, a widening shelf, and the offshore Agulhas Current, the index area is subject to a variety of processes. The analysis was confined to the period 2006–2017, when high resolution satellite coverage of the shelf zone facilitates analysis of SST, winds and currents. The coastal hydrology was described by CHIRPS v2 rainfall (5 km resolution; Funk et al 2015), CMORPH satellite rainfall (25 km; Joyce et al. 2004) and SADW discharge records for the Gamtoos, Sundays and Fish Rivers. The marine variables include: SST, sea level air pressure (SLP), winds, heat and radiation fluxes, salinity, currents, vertical motion (cf. Table 1). An 8-day resolution compatible with MODIS chlorophyll fluorescence yields a record length of 552 comprised of 46 x 12 years (1 Jan 2006 - 31 Dec 2017). From this, multi-day events were identified by ranking the index-area chlorophyll fluorescence and salinity at 10 m depth. The chlorophyll fluorescence time series was subjected to wavelet spectral analysis to determine the degree of cyclicity and its amplitude and period.

Statistical associations were studied by pair-wise correlation of the mean annual cycle of chlorophyll fluorescence and 10 m salinity with a variety of environmental parameters listed in Table 1. Statistical significance above 90% confidence was achieved with the Pearson-product moment r > |0.62| for 6 degrees of freedom. Relationships with chlorophyll fluorescence motivated a point-to-field correlation analysis of the salinity record and large scale fields of Oct-Mar sea level air pressure, covering 25–45S, 10–43E, 2006-2017. A composite average of the top-10 chlorophyll fluorescence events was conducted to study anomaly patterns for 500 hPa geopotential height, satellite rainfall and surface zonal winds. Composite maps were analyzed sequentially at -4, -3, -2, -1, 0 days before the time of peak ocean colour, to reveal the large scale atmospheric forcing. The top-10 events began on the following dates: 1 Nov 2009, 1 Nov 2014, 24 Oct 2014, 24 Oct 2009, 17 May 2015, 19 Dec 2007, 9 Nov 2014, 23 Oct 2012, 10 Feb 2011, 23 Apr 2015, ranked by value. Exploratory analysis of Agulhas Current pulses (cf. Appendix Fig A2), were made by calculating HYCOM daily sea surface height variance 2006-2017 per 0.1° longitude bin from 24-29E on 34.5S, and via case study hovmoller sequences across the shelf.

Inter-annual fluctuations of commercial fisheries and environmental conditions were explored using monthly ocean reanalysis appropriate for longer time scales: Jan-Jun season SODA v3 ocean reanalysis (Carton et al. 2018), satellite SST (Chin et al. 2017), and annual catch data from local and international sources (van Zyl and Willemse 2000, J. Coetzee pers. comm. 2018). Pair-wise correlations were calculated for the main fishery species in the period 1981-2015; 90% confidence is reached with r > |0.40| for 35 degrees of freedom. The websites used for data extraction and analysis are listed in the acknowledgements.

3. Results

3.1 Marine climate and annual cycle

Mean maps of the study area topography and SST are illustrated in Fig 1a,b. Sharp gradients in the mean SST field were evident: inshore waters are 17-19C while offshore waters are 22-24C. Shelf-edge upwelling next to the warm Agulhas Current divided the two regimes (Lutjeharms et al. 2000, Malan et al. 2018). Over the cool inshore waters, the sensible heat flux was low (Fig 1c) and the atmospheric boundary layer was shallow (800 m). So the coastal topography steers the wind to a longshore axis (Schumann and Martin 1991)

https://doi.org/10.5194/os-2019-55
Preprint. Discussion started: 5 August 2019

that further sharpens the gradients.

Figure 1d-f illustrates the mean annual cycle of key variables. Chlorophyll fluorescence showed bi-modal peaks in Oct-Nov and Mar-Apr, of importance to the marine food web and fishery abundance (Shannon et al. 1984, Hutchings 1994). The wind stress curl reached a cyclonic condition from Oct-Mar that favoured upwelling via easterly wind shear attending sub-tropical high pressures. During winter season, anticyclonic curl via westerly wind shear promoted downwelling. The annual cycle of 10 m salinity revealed a summer minimum, induced by rainfall and river discharge from November to March. A histogram of daily zonal winds (Fig 1g) showed near equal occurrence of upwelling (-U) and downwelling favourable conditions, and many instances of 5-10 m/s in both east and west sectors. A case study upwelling event with high chlorophyll fluorescence 24 Oct - 8 Nov 2009 is illustrated in the appendix (Fig A1), and links easterly winds, rainfall and marine productivity.

3.2 Chlorophyll and water flux

The mean MODIS chlorophyll and fluorescence maps (Fig 2a,b) show higher values inshore and around the capes, and lower values outside of the Agulhas Current. The chlorophyll tended to hug the coastal zone and its wave- and river- suspended sediments. In contrast the fluorescence exhibited an offshore plume from Cape Padrone, associated with shelf-edge upwelling. The chlorophyll fluorescence index-area time series (Fig 2c) is punctuated by spikes of 10 mg/m^3, which identify key events mainly at the beginning and end of summer. Its wavelet spectral energy (Fig 2d) exhibited fluctuations from 20 to 45 days in early and late summer bursts. The years 2009-2011 experienced greater 20-50 day pulsing, while 80-90 day oscillations of chlorophyll fluorescence characterized the years 2014-2015 and 2017. At 8-day resolution, higher frequencies were unresolved.

The mean HYCOM water flux into the ocean (Fig 3a) exhibited a low axis along the shelf edge. Marine rainfall was a feature outside and east of the Agulhas Current. Significant river discharges on the upstream coast and in the bays were measured (Fig 3b). The Gamtoos-Sundays River output was 1-10 m^3/s; while the Fish River reached ~ 100 m^3/s during wet spells. Yet there were prolonged dry spells characterized by minimal discharge. The case study section considers seasonal changes from 2010 to 2011 and a detailed analysis of an event in 2014.

3.3 Case study productivity and salinity events

The river discharge time series reflects a period of change from dry to wet conditions from Aug 2010 to Mar 2011. Rainfall maps for those contrasting periods (Fig 3c,d) exhibited

https://doi.org/10.5194/os-2019-55
Preprint. Discussion started: 5 August 2019

dry conditions over the Eastern Cape followed by widespread rainfall. River discharges rose from 1 m^3/s to ~100 m^3/s; and the shelf exhibited increased chlorophyll (Fig 3e,f). The main axis of the Agulhas Current was inshore early in the event and shifted seaward later in the event. Initially there was northeastward flow along the coast that diminished later.

Figure 4a-g follows the development of a low salinity event from 15-30 Oct 2014. Initially there was salty water over the shelf, but gradually the upstream rainfall and river discharges (~35 m^3/s) fed southwestward into a buoyant plume. By the end of Oct 2014, the near-surface salinity over the shelf declined to 35.0 ppt. The daily 10 m salinity record reveals this event to be the lowest in a decade. The large-scale wind map shows SE flow over South Africa, driven onshore by a trough in the Mozambique Channel and a mid-latitude high pressure cell (Fig 4e). Subsequently, there was a noteworthy increase in chlorophyll from mid-October to early November 2014 (Fig 4f,g). An increase in upstream rainfall and run-off promoted water turbidity and marine productivity.

Vertical sections of zonal wind, currents and sea temperature are shown in Fig 5a-c averaged over the high chlorophyll event (17 Oct - 8 Nov 2014). Along the 26E longitude these sections identify the easterly low level jet over the shelf and associated cyclonic wind shear. The upwelling-favourable easterly winds were vertically capped at 850 hPa (1.5 km). The wind stress vorticity was ~ 10^{-6} N m^{-3}, lifting water near the coast. The vertical section of zonal currents revealed a westward Agulhas Current of 1.4 m/s between 34.7-34.3S latitude. Near the coast zonal currents were zero, hence the cyclonic vorticity at 34.2S was ~ 3 10^{-5} s^{-1}, lifting water at the shelf edge. The sea temperature section exhibited warm 21C sea temperatures offshore, typical of the Agulhas Current during spring. Inshore there was pronounced upwelling of 12C water lifted from ~ 80 m depth at 34.1S, breeching the surface with a temperature of 14C.

Vertical motion is generated by vorticity of the longshore wind stress and current (Hsueh and O'Brien 1971, Gill and Schumann 1979, Blanton et al. 1981, Brink 1998) according to: $\zeta\tau / \rho f = W = \zeta_{U10} (C_D Z / f dt)$. Using the above vorticity values, water density (ρ) 10^3 kg m^{-3}, coriolis (f) 7.7 10^{-5} s^{-1}, bottom drag (C_D) 10^{-2} (Liu and Gan 2015), depth of current shear (Z) 2 10^2 m, over a multi-day time (dt) 10^5 s. The wind stress curl and the current shear each generate vertical motion of ~ 10^{-5} m/s. In the 2014 case study, the easterly winds and currents combined to lift water off Cape Padrone. Yet half of the time winds are from the west (cf. Fig 1g) and oppose the current-induced upwelling.

An exploratory analyses of processes underpinning shelf-edge upwelling was made. Appendix Fig A2 illustrates that variance of sea surface height is greatest outside the Agulhas

https://doi.org/10.5194/os-2019-55
Preprint. Discussion started: 5 August 2019

Current. Hovmoller plots of sea surface height during peak chlorophyll fluorescence events exhibited gradual strengthening of the cross-shelf gradient, as pulses of +SSH moved westward at ~0.2 m/s outside the Agulhas Current and wind-driven offshore Ekman transport induced −SSH inshore.

3.4 Statistical insights

The statistical analysis of temporal records reveals a link between coastal rainfall > 10 mm/day and chlorophyll (Fig 6a) particularly in summer (r > 0.6) when run-off is greater. According to the point-to-field correlation map (Fig 6b), reduced salinity during summer is associated with a low pressure trough over the Benguela and a high pressure in the mid-latitudes southeast of Africa, which together promote upwelling favourable easterly winds. The correlation map with respect to sea surface height anomalies (Fig 6c), shows that reduced salinity is linked with a low-inshore / high-offshore gradient, hence accelerated shelf-edge currents and shear-induced upwelling.

Figure 7 illustrates a sequence of composite 500 hPa geopotential height anomalies for the top 10 chlorophyll fluorescence events. The maps follow the eastward movement of a mid-latitude ridge, from 4 days before, to the day of maximum colour in the index area. The ridge moved 10° longitude per day on 50S, and generated easterly wind anomalies of 10 m/s on the shelf edge and heavy rainfall over the Eastern Cape interior. Hence large-scale weather conditions promoted marine productivity through the concurrence of upwelling and river discharge.

Table 1 lists the pair-wise cross-correlation between the mean annual cycle of chlorophyll, salinity and other variables from the index area. Chlorophyll fluorescence is most correlated with salinity (r = -0.62) followed by meridional and zonal current (-0.56). Processes that enhance chlorophyll fluorescence over the annual cycle are water mass freshening and an intensified Agulhas Current (cf. Fig 6c, Fig A2). For salinity, annual cycle correlations were generally higher. The strongest relationships were with sea level air pressure (r = 0.91), net longwave radiation (0.91) and wave height (0.90), indicating that lower air pressure, less outgoing radiation (eg. greater cloudiness) and smaller wave height coincided with lower salinity over the annual cycle.

Annual fish catch data (Fig 8) provide a basis to evaluate environmental influences, as listed in Table 2. Year-to-year changes of squid, anchovy and sardine catch displayed weak relationships with many marine variables. Only squid catch exhibited inter-annual variability; anchovy catch was minuscule and sardine catch showed decadal oscillations. Negative

https://doi.org/10.5194/os-2019-55
Preprint. Discussion started: 5 August 2019

(southwestward) currents and diminished heat fluxes favoured squid catch. Anchovy and sardine catch increased following a season with anomalous upper northerly wind (V 2, r = -0.37), consistent with the large-scale summer-time weather patterns in Fig 6c that underpin increased productivity (cf. Jury 2011, Fig 5 therein).

4. Discussion and conclusion

The relative role of local and remote atmosphere and ocean forcing on marine productivity over the shelf near Cape St Francis has been explored. The 8-day MODIS chlorophyll fluorescence and HYCOM salinity in the period 2006-2017 were the primary descriptors in an index-area 34.5-33.75S, 24-26.5E. A variety of atmospheric and oceanic variables were obtained from high resolution reanalysis products such as HYCOM, and annual cycle correlations were explored.

It was recognized that ocean colour, as a proxy for marine productivity, has uncertainties due to potential contamination by clouds and aerosols, and by coastal wave- and river- induced sediments. This uncertainty was addressed by the addition of red-band fluorescence line height to the traditional green-band chlorophyll concentration. Over the annual cycle, salinity and ocean currents exhibited significant negative relationships with chlorophyll fluorescence. Furthermore, it was also recognized that the ocean reanalysis are based on coupled data assimilation that benefits from satellite technology but limited insitu calibration. Although the work infers that the ocean reanalysis is equivalent to reality, there is uncertainty that limits understanding. This does not prevent explorational studies as reported here, but could inhibit translating outcomes into strategic decisions.

The mean pattern of chlorophyll fluorescence revealed an axis of high values off Cape Padrone, where current-edge upwelling is prevalent (Swart and Largier 1987, Lutjeharms et al. 2000, Lutjeharms 2006 pp.140-146). Downstream widening of the shelf bathymetry elongates this cold tongue toward the wind-driven upwelling plumes off Cape Recife and Cape St Francis. This shelf-edge feature modulates the location of stable layers and primary production. From October to March, a strong vertical temperature gradient tends to concentrate phytoplankton at depths > 30 m (Probyn et al. 1994), at the bottom of the euphotic zone and wind mixed layer.

The annual cycle analysis presented here revealed that marine productivity peaked in early and late summer when sub-tropical cut-off lows were most frequent (Favre et al. 2013). The large-scale point-to-field analysis indicated that a mid-latitude high pressure ridge underpins marine productivity, reducing salinity via upstream rainfall / coastal run-off and promoting wind-driven coastal upwelling and cross-shelf SSH gradients that accelerate shelf-

https://doi.org/10.5194/os-2019-55
Preprint. Discussion started: 5 August 2019

edge currents and upwelling. Case studies and the top-10 composite revealed similar features in chlorophyll fluorescence events: they follow a spell of sustained easterly wind-driven coastal upwelling and low salinity induced by local and upstream rainfall and river discharge. The competing influences of: i) coastal run-off ~100 m^3/s, ii) marine rainfall, iii) air-sea interactions, iv) inshore upwelling ~10 m/day, and v) intrusions from offshore; can not be resolved in this exploratory work and deserve further study. Yet the evidence during productivity events indicates that cyclonic shear of easterly winds and shelf-edge currents (cf. Fig 5a,b, Fig 6c, Fig A2) play prominent roles to lift water and generate high chlorophyll fluorescence along the coast. Statistically, about half the time westerly winds oppose the currents and suppress marine productivity, mainly during winter.

Earlier findings on multi-day upwelling events (Goschen et al. 2012) appear complimentary to those reported here for co-varying indices of marine productivity. High chlorophyll fluorescence lags a few days behind cyclonic wind and current shear and the upstream coastal hydrology, which shares a common atmospheric driver. Environmental controls on inter-annual fluctuations of the commercial fishery were explored using ocean reanalysis appropriate for longer time scales (monthly SODA3). Southwestward currents and diminished heat fluxes favoured squid catch, while anchovy and sardine were linked with upper northerly wind, and large-scale weather patterns that underpin coastal upwelling and river discharge (cf. Jury 2011). Earlier work determined physiographic preferences for pelagic fish on the East Agulhas Bank (Armstrong et al. 1991), some of which are reflected in the results of Table 2 here. Further work will analyze the pulsing of the Agulhas Current and its affect on environmental conditions over the shelf from intra-seasonal to multi-year time scales.

Acknowledgements

Most environmental data were sourced from websites of the International Research Institute for Climate, Climate Explorer of the Netherlands Meteorological Institute, NASA Giovanni, and University of Hawaii Asia-Pacific Data Resource Center. Fish catch derived from Fishbase, supplemented by South African government sources. River discharge data were obtained from the South African Dept of Water, Hydrology Services website.

References

Armstrong, M.J., Chapman, P., Dudley, S.F.J., Hampton, I. and Malan, P.E.. Occurrence and population structure of pilchard, round-herring and anchovy off the east coast of southern Africa. S. Afr. J. Marine Science. 11: 227–249, 1991.

Beckley, L.E. Spatial and temporal variability in sea temperatures in Algoa Bay, South Africa. S. Afr. J. Science. 84: 67–69. 1988.

https://doi.org/10.5194/os-2019-55
Preprint. Discussion started: 5 August 2019

Blanton, J.O., Atkinson, L.P., Pietrafesa, L.J. and Lee, T.N. The intrusion of Gulf Stream water across the continental shelf due to topographically-induced upwelling. Deep-Sea Res. 28A: 393–405. 1981.

Brink, K.H. Wind-driven currents over the continental shelf. In: Brink KH, Robinson AR (eds), The Sea vol. 10. The global coastal ocean: processes and methods. New York: John Wiley & Sons. pp 3–20. 1998.

Carton, J.A., Chepurin, G.A. and Chen, L. SODA3 a new ocean climate reanalysis, J. Climate 31: 6967–6983. 2018.

Chassignet, E.P., Hurlburt, H.E., Metzger, E.J., Smedstad, O.M., Cummings, J.A., Halliwell, G.R., Bleck, R., Baraille, R., Wallcraft, A.J., Lozano, C., Tolman, H.L., Srinivasan, A., Hankin, S., Cornillon, P., Weisberg, R., Barth, A., He, R., Werner, R., and Wilkin, J. US GODAE: Global ocean prediction with the Hybrid coordinate ocean model (Hycom). Oceanography 22: 64–75. 2009.

Chin, T.M., Vazquez-Cuervo, J., Armstrong, E.M., A multi-scale high-resolution analysis of global sea surface temperature, Remote Sens. Environ. 200: 154−169. 2017.

Cochrane, K.L., Oliver, B. and Sauer, W. An assessment of the current status of the chokka squid fishery in South Africa and an evaluation of alternative allocation strategies. Marine Policy, 43: 149–163. 2014.

Cummings, J.A. and Smedstad, O.M. Variational data assimilation for the global ocean. Data assimilation for atmospheric, oceanic and hydrologic applications II, chapter 13: 303–343. 2013.

Favre, A., Hewitson, B., Lennard, C., Cerezo-Mota, R., Tadross, M. Cut-off Lows in the South Africa region and their contribution to precipitation. Climate Dyn. 41: 2331–2351. 2013.

Funk, C., Peterson, P., Landsfeld, M., Pedreros, D., Verdin, J., Shukla, S., Husak, G., Rowland, J., Harrison, L., Hoell, A., and Michaelsen, J. The climate hazards infrared precipitation with stations: a new environmental record for monitoring extremes, Nature Sci. Data, 2, 150066. 2015.

Gelaro, R., McCarty, W., Suárez, M.J., Todling, R., Molod, A., Takacs, L., Randles, C.A., Darmenov, A., Bosilovich, M.G., Reichle, R., Wargan, K., Coy, L., Cullather, R., Draper, C., Akella, S., Buchard, V., Conaty, A., da Silva, A.M., Gu, W., Kim, G., Koster, R., Lucchesi, R., Merkova, D., Nielsen, J.E., Partyka, G., Pawson, S., Putman, W., Rienecker, M., Schubert, S.D., Sienkiewicz, M., and Zhao, B. The Modern-era retro-spective analysis for research and applications, version 2 (MERRA2). J. Climate, 30, 5419–5454. 2017.

Gill, A.E. and Schumann, E.H. Topographically induced changes in the structure of an inertial coastal jet: application to the Agulhas Current. J. Phys. Oceanogr. 9: 975–991. 1979.

Goschen, W.S. and Schumann, E.H. Ocean current and temperature structures in Algoa Bay and beyond during November 1986. S. Afr. J. Marine Science 7: 101−116. 1988.

Goschen, W.S. and Schumann, E.H. Agulhas Current variability and inshore structures off the Cape Province, South Africa. J. Geophys. Res. 95: 667–678. 1990.

Goschen, W.S. and Schumann, E.H. The physical oceanographic processes of Algoa Bay, with emphasis on the western coastal region. SAEON internal publication, Pretoria: 84 pp. 2011.

Goschen, W.S., Schumann, E.H., Bernard, K.S., Bailey, S.E. and Deyzel, S.H.P. Upwelling and ocean structures off Algoa Bay and the south-east coast of South Africa, Afr. J. Marine Science 34: 525–536. 2012.

Goschen, W.S., Bornman, T.G., Deyzel, S.H.P. and Schumann, E.H. Coastal upwelling on the far eastern Agulhas Bank associated with large meanders in the Agulhas Current. Cont. Shelf Res. 101: 34–46. 2015.

Gower, J. On the use of satellite-measured chlorophyll fluorescence for monitoring coastal waters, Intl. J. Remote Sensing, 37, 2077-2086. 2016.

Houskeeper, H.F. and Kudela, R.M. Behind the masks in coastal ocean color, Ocean Optics Conference, <oceanopticsconference.org/extended/Houskeeper_Henry.pdf> 2017.

https://doi.org/10.5194/os-2019-55
Preprint. Discussion started: 5 August 2019

Hsueh Y and O'Brien JJ. Steady coastal upwelling induced by an along-shore current. J. Phys. Oceanogr. 1: 180–186. 1971.

Hu, C., Lee, Z. and Franz, B. Chlorophyll-a algorithms for oligotrophic oceans: A novel approach based on three-band reflectance difference. J. Geophys. Res. 117: doi10.1029/2011jc007395. 2012.

Hutchings, L. The Agulhas Bank: a synthesis of available information and a brief conmparison with othe east-coast shelf regions. S. Afr. J. Science 90: 179−185. 1994.

Joyce. R.J., Janowiak, J.E., Arkin, P.A. and Xie, P.P. CMORPH: A method that produces global precipitation estimates from passive microwave and infrared data at high spatial and temporal resolution. J. Hydrometeorol. 5: 487–503. 2004.

Jury, M.R., MacArthur, C. and Reason, C. Observations of trapped waves in the atmosphere and ocean along the coast of southern Africa. S. Afr. Geogr. J. 72: 33–46. 1990.

Jury, M.R. Environmental influences on South African fish catch: South coast transition, Intl. J. Oceanography, doi10.1155/2011/920414. 2011.

Jury, M.R. and Goschen, W. Inter-relationships between physical ocean-atmosphere variables over the shelf south of South Africa from reanalysis products, Cont. Shelf Res. (in review). 2019.

Liu, Z. and Gan, J. Upwelling induced by the frictional stress curl and vertical squeezing of the vortex tube over a submerged valley in the East China Sea, J. Geophys Res. Oceans 120: 2571–2587. 2015.

Lutjeharms, J.R.E. The Agulhas Current. Berlin: Springer. 329 pp. 2006.

Lutjeharms, J.R.E, and Roberts, H.R. The Natal Pulse: an extreme transient on the Agulhas Current. J. Geophysical Res. 93: 631–645. 1988.

Lutjeharms, J.R.E., Catzel, R. and Valentine, H.R. Eddies and other boundary phenomena of the Agulhas Current. Cont. Shelf Res. 9: 597–616. 1989.

Lutjeharms, J.R.E., Cooper, J., Roberts, M.J. Upwelling at the inshore edge of the Agulhas Current. Cont. Shelf Res. 20: 737–761. 2000.

Malan, N., Backeberg, B., Biastoch, A., Durgadoo, J.V., Samuelsen, A., Reason, C., Hermes, J. Agulhas Current Meanders facilitate shelf - slope exchange on the Eastern Agulhas Bank. J. Geophys. Res. Oceans 123: 4762−4778. 2018.

Pattrick, P., Strydom, N.A. and Goschen, W.S. Shallow-water, nearshore current dynamics in Algoa Bay, South Africa, with notes on the implications for larval fish dispersal. Afr. J. Marine Science 35: 269−282. 2013.

Probyn, T.A., Mitchell-Innes, B.A., Brown, P.C., Hutchings, L. and Carter, R.A., A review of primary production and related processes on the Agulhas Bank. S. Afr. J. Sci. 90: 166–173. 1994.

Reichle, R.H., Draper, C.S., Liu, Q., Girotto, M., Mahanama, S.P., Koster, R.D. and DeLannoy, G.J. Assessment of MERRA-2 land surface hydrology estimates, J. Climate 30: 2937–2960. 2017.

Roberts, M.J. Coastal currents and temperatures along the eastern region of Algoa Bay, South Africa, with implications for transport and shelf-bay water exchange. Afr. J. Marine Science 32: 145−161. 2010.

Roberts, M.J., Downey, N.J. and Sauer, W.H. The relative importance of shallow and deep shelf spawning habitats for the South African chokka squid. ICES J. Marine Science 69: 563–571. 2012.

Roualt, M. and Lutjeharms. J.R.R. Estimation of sea-surface temperature around southern Africa from satellite-derived microwave observations. S. Afr. J. Science 99: 489−494. 2003.

Rouault, M.J., and Penven, P. New perspectives on Natal Pulses from satellite observations. J. Geophys. Res. 116: 1–14. 2011.

Scharler, U.M. and Baird, D. The filtering capacity of selected Eastern Cape estuaries, South Africa. Water S.A. 31: 483-490. 2005.

https://doi.org/10.5194/os-2019-55
Preprint. Discussion started: 5 August 2019

Ocean Science Discussions
Open Access

Schumann, E.H., Perrind, L.A. and Hunter, I.T. Upwelling along the south coast of the Cape Province, South Africa. S. Afr. J. Science 78: 238−242. 1982.

Schumann, E.H. The bottom boundary layer inshore of the Agulhas Current off Natal in August 1975. S. Afr. J. Marine Science 4: 93–102. 1986.

Schumann, E.H. The coastal ocean off the east coast of South Africa. Trans. Royal Soc. S. Afr. 46: 215–228. 1987.

Schumann, E.H. Wind-driven mixed layer and coastal upwelling processes off the south coast of South Africa. J. Marine Research 57: 671–691. 1999.

Schumann, E.H., and Brink, K.H. Coastal trapped waves off the coast of South Africa: generation, propagation and current structures. J. Phys. Oceanogr 20: 1206–1218. 1990.

Schumann, E.H. and Martin, J.A. Climatological aspects of the coastal wind field at Cape Town, Port Elizxabeth and Durban. S. Afr. Geographical J. 73: 48−51. 1991.

Schumann, E.H., Churchhillm J.R.S. and Zaayman, H.J. Oceanic variability in the western sector of Algoa Bay, South Africa. Afr. J. Marine Science 27: 65−80. 2005.

Shannon, L.V., Hutchings, L., Bailey, G.W., Shelton, P.A. Spatial and temporal distribution of chlorophyll in southern African waters as deduced from ship and satellite measurements and their implications for pelagic fisheries. S. Afr. J. Marine Science 2: 109-130. 1984.

Swart, V.P. and Largier, J.L. Thermal structure of Agulhas Bank water. In: Payne AIL, Gulland JA, Brink KH (eds), The Benguela and comparable ecosystems. S. Afr. J. Marine Science 5: 243–253. 1987.

Tolman, HL. User manual and system documentation of WAVEWATCH-III. NCEP Technical Note, Washington, 139 pp. 2002.

van Bladeren, D., Zawada, P.K. and Mahlangu, D. Statistical based regional flood frequency estimation study for South Africa using systematic, historical and palaeo-flood data. Water Research Commission W.R.C. Report 1260/1/70. 2007.

van Zyl, B. and Willemse, N.E. FishBase: a database and fisheries management-oriented tool for the 21st century, African J. Aquatic Sci. 25: 225–226. 2000.

https://doi.org/10.5194/os-2019-55
Preprint. Discussion started: 5 August 2019

Table 1 Pair-wise correlation values for the mean annual cycle averaged over the index area, 2006-2017. N=46 at 8-day resolution; significant values are bold.

	Chloro	*Salt*	
Chloro			Chlorophyll+fluorescence
Salt	**-0.62**		Salinity at 10 m depth
SST	0.34	**-0.89**	Sea surface temperature
U wind	-0.30	**0.83**	Zonal wind at 10 m height
SLP	-0.29	**0.91**	Sea level air pressure
LHF	-0.15	**0.74**	Evaporation (latent heat flux)
SHF	-0.45	0.25	Sensible heat flux
Q_s	0.01	**-0.71**	Net shortwave radiation
Q_L	-0.43	**0.91**	Net longwave radiation
curl	0.32	**-0.76**	Vorticity of wind stress
wv ht	-0.27	**0.90**	Wave height (sig.)
wv dir	-0.30	**0.63**	Wave direction
wv per	-0.21	**0.70**	Wave period
U 10 cur	-0.56	0.59	Zonal current at 10 m depth
V 10 cur	-0.55	**0.79**	Meridional current at 10 m
W 30	0.36	-0.55	Vertical motion at 30 m depth

Table 2 Pair-wise correlation of annual fish catch in the outer domain (cf. Fig 8) and Jan-Jun marine data averaged over the index area, 1981-2015. N=35 at 1-yr resolution; significant values are bold. Variables are same as in Table 1, except Temp = sea temp at 10 m depth, U2 / V2 wind = upper level wind (200 hPa).

	Squid	*Anchovy*	*Sardine*
Squid			
Anchovy	-0.01		
Sardine	0.29	**0.44**	
SST	0.21	0.18	0.14
Temp	-0.07	**0.44**	0.26
Salt	0.13	0.31	0.30
SLP	0.15	-0.17	-0.01
U wind	-0.14	0.29	0.07
V wind	-0.30	0.22	-0.13
U cur	**-0.54**	-0.09	-0.06
V cur	**-0.58**	0.15	-0.01
LHF	**-0.46**	-0.03	-0.29
SHF	-0.35	-0.09	-0.35
Qs	-0.08	-0.20	-0.05
Q_L	-0.28	-0.08	-0.19
curl	0.03	-0.29	-0.20
U 2	-0.23	0.31	0.18
V 2	-0.04	-0.38	-0.37
rain	0.22	0.07	0.21

https://doi.org/10.5194/os-2019-55
Preprint. Discussion started: 5 August 2019

Ocean Science
Discussions
Open Access

Figures

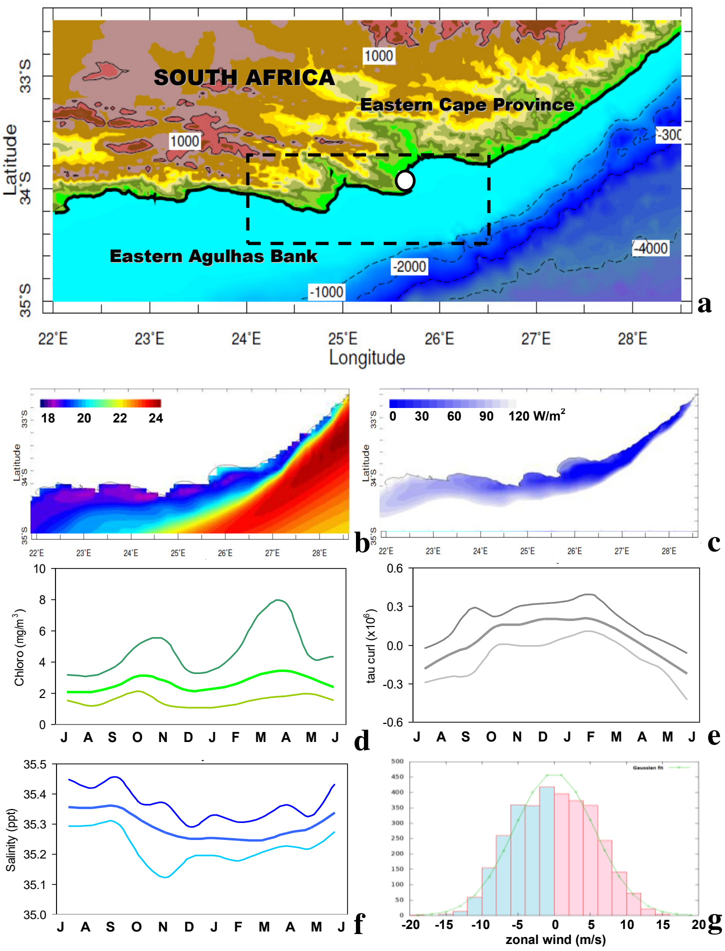

Figure 1 (a) Topography of the outer study domain (and dashed index area), shelf bathymetry and Port Elizabeth (dot). Mean maps 2006-2017 of HYCOM reanalysis (b) SST (°C) and (c) net heat flux (shaded < 120 W/m^2). Index-area mean annual cycle of: (d) chlorophyll fluorescence, (e) wind stress curl, and (f) salinity; with upper / lower 2.5 percentiles, summer is unified. (g) Histogram of index-area daily zonal wind, (blue–from east / red–from west).

https://doi.org/10.5194/os-2019-55
Preprint. Discussion started: 5 August 2019

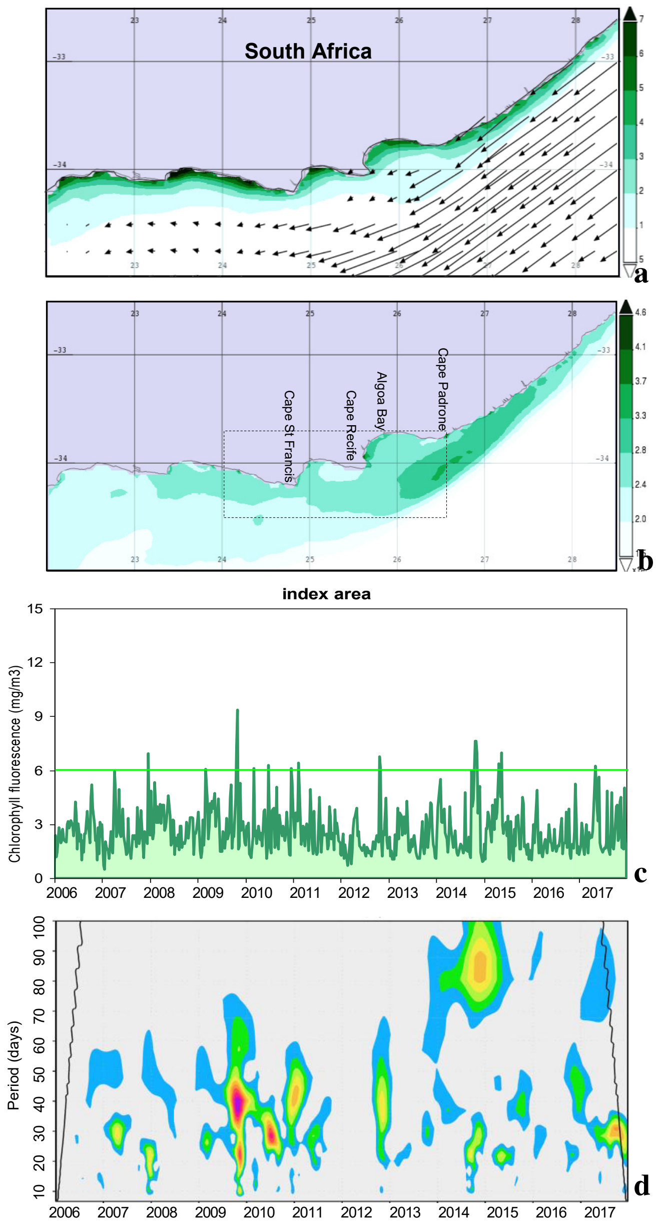

Figure 2 MODIS 2006-2017 mean: (a) chlorophyll concentration (mg/m^3) with SODA3 mean near-surface currents, (b) fluorescence line height (W/m^2) and index-area. (c) Time series of 8-day index-area chlorophyll fluorescence; composite cases > 6 mg/m^3. (d) Wavelet spectra energy of the time series, shaded from 90% to 99% confidence.

https://doi.org/10.5194/os-2019-55
Preprint. Discussion started: 5 August 2019

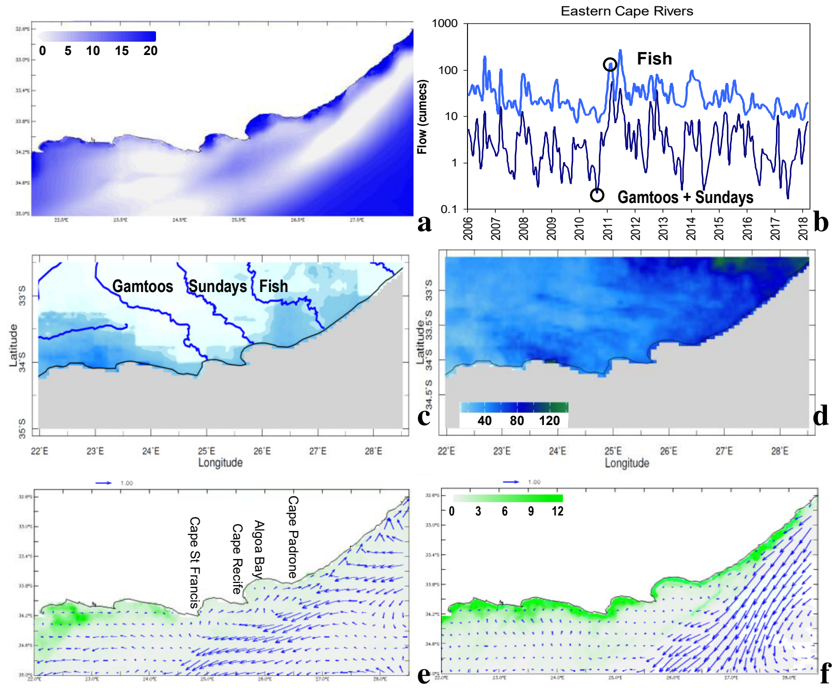

Figure 3 (a) Mean 2006-2017 HYCOM water flux into ocean (mm/day). (b) Observed monthly river discharge at the coast, with dry spell 1-10 Aug 2010 and wet spell 1-10 Mar 2011 (circled). (c,d) CHIRPS coastal rainfall (cumulative, mm), (e,f) MODIS chlorophyll (shading) and HYCOM near-surface current vectors during the dry spell (left) and wet spell. (c) illustrates the main rivers.

https://doi.org/10.5194/os-2019-55
Preprint. Discussion started: 5 August 2019

Ocean Science
Discussions
Open Access
EGU

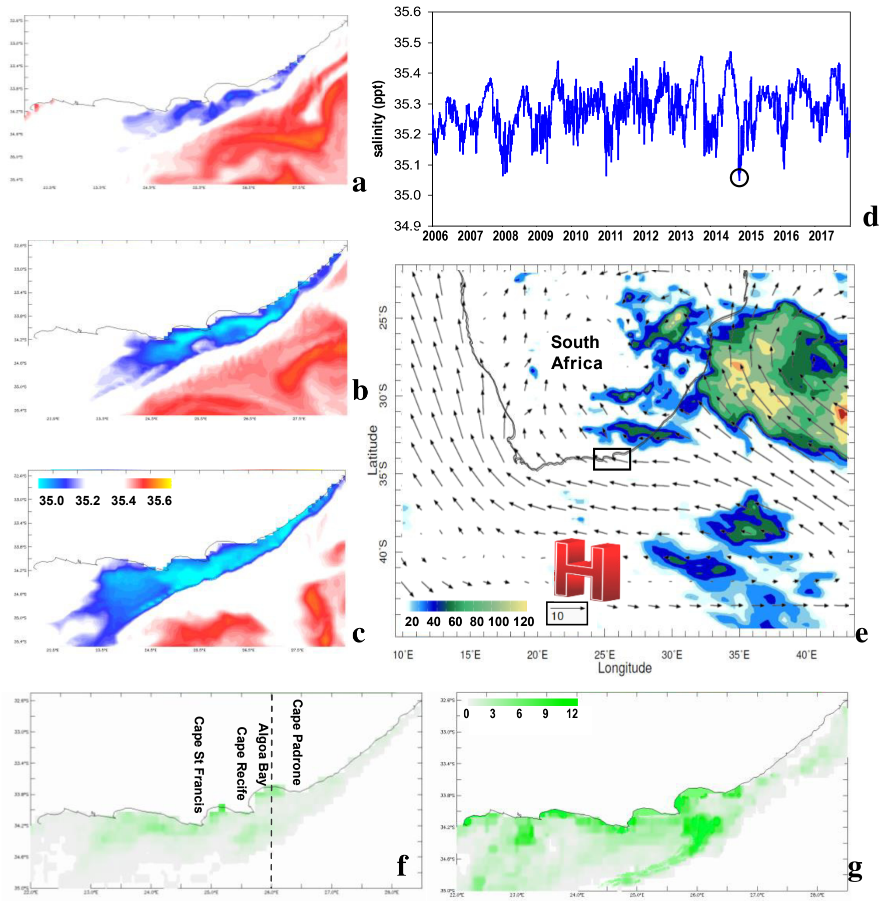

Figure 4 Salinity maps (a) 15-20 Oct, (b) 20-25 Oct, (c) 25-30 Oct 2014, when the cumulative Fish River discharge exceeded 10^{10} m^3. (d) Daily record of index-area 10 m salinity, with case study circled. (e) Large-scale 15-25 Oct 2014 cumulative CMORPH rainfall (shaded, mm) and low level winds (vector). MODIS chlorophyll: (f) 8-23 Oct, and (g) 24 Oct - 8 Nov 2014. Dashed line in (f) is the section in Fig 5.

https://doi.org/10.5194/os-2019-55
Preprint. Discussion started: 5 August 2019

Ocean Science
Discussions
Open Access
EGU

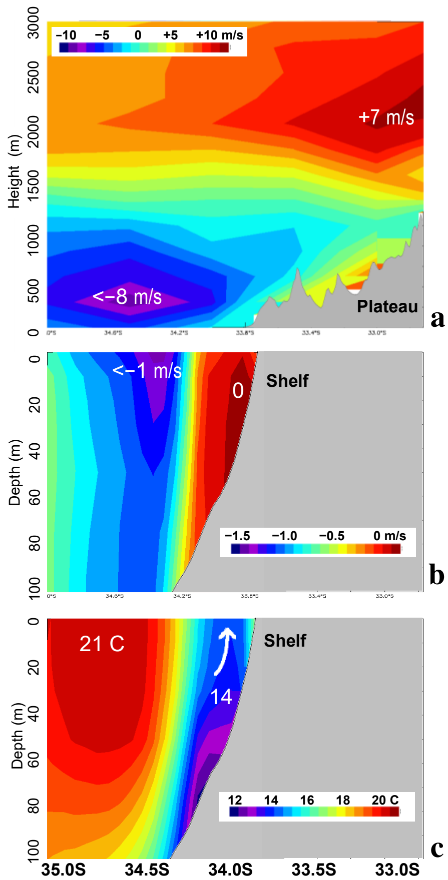

Fig 5 Vertical N-S sections on 26E averaged 15 Oct - 5 Nov 2014 of: (a) MERRA2 zonal wind, (b) HYCOM zonal current, and (c) sea temperature.

https://doi.org/10.5194/os-2019-55
Preprint. Discussion started: 5 August 2019

Ocean Science
Discussions

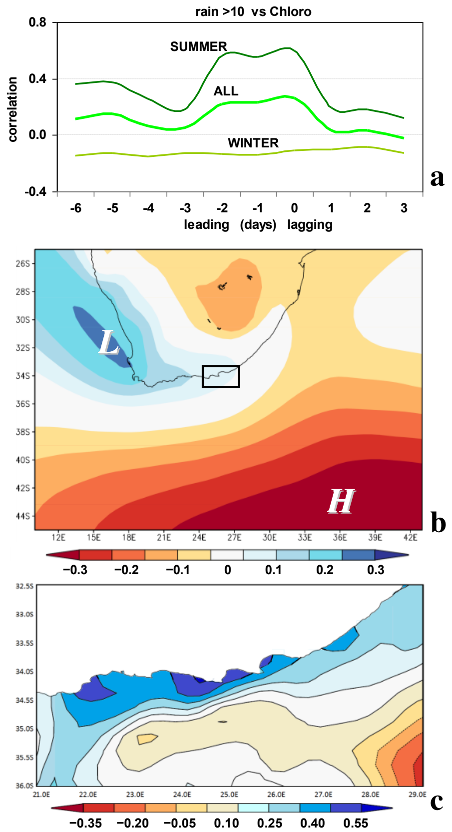

Figure 6 (a) Lag-correlation between index-area coastal rainfall > 10 mm/day and chlorophyll fluorescence N=102, for summer/ all/ winter season. (b) Point-to-field correlation of salinity index (cf. Fig 4d) and summer-season field at 3-day lead, Oct-Mar 2006-2017 sea-level air pressure, icons given w.r.t. lower salinity. (c) Same point-to-field correlation except with sea-surface height anomalies, shaded w.r.t. lower salinity (eg. low-inshore).

https://doi.org/10.5194/os-2019-55
Preprint. Discussion started: 5 August 2019

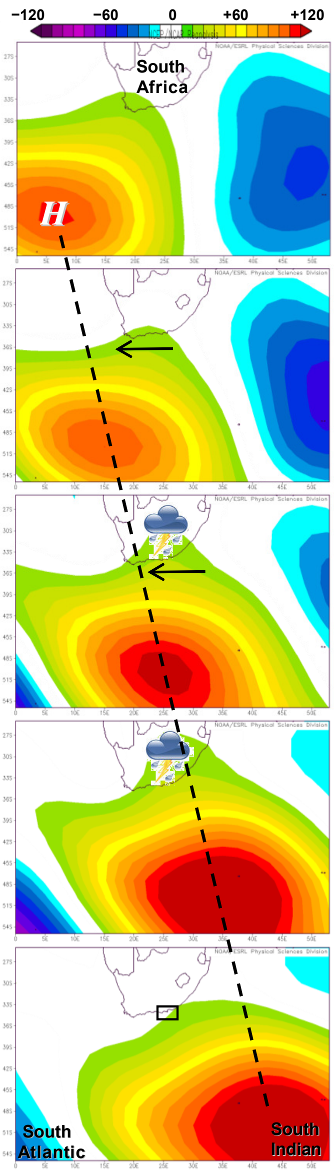

Figure 7 Composite 500 hPa geopotential height anomalies (shaded) for the top 10 chlorophyll fluorescence events, (top-down) from -4 days (before) to zero (colour max), with dashed line following the mid-latitude ridge. Composite anomaly easterly winds (>10 m/s) and heavy rainfall (>50 mm) are represented by arrow and icon.

https://doi.org/10.5194/os-2019-55
Preprint. Discussion started: 5 August 2019

Ocean Science
Discussions

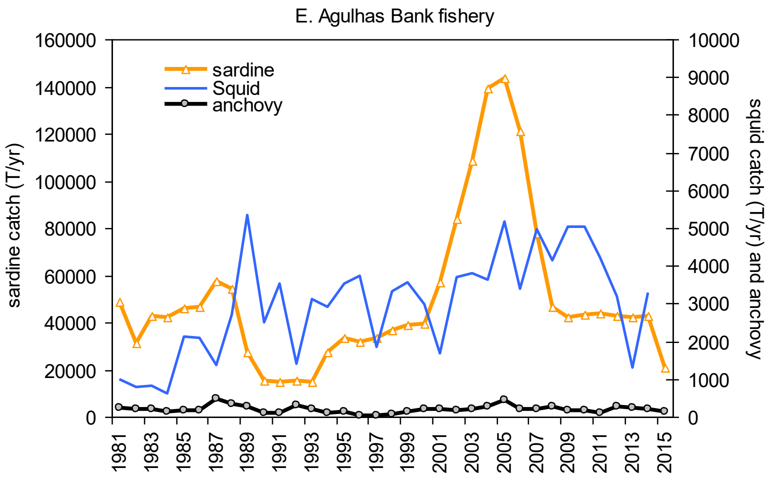

Figure 8 Time series of annual catch for leading fisheries in the eastern Agulhas Bank (outer domain, cf. Fig 1a,2b); the basis for results in Table 2.

https://doi.org/10.5194/os-2019-55
Preprint. Discussion started: 5 August 2019

Ocean Science
Discussions
Open Access

Appendix

Acronyms, dataset and horizontal resolution.

	Name	Horiz. Resolution
CHIRPS	Climate Hazards InfraRed Precipitation with Station v2	5 km
CMORPH	CPC Morphed polar- and geostationary- satellite rainfall	25 km
HYCOM	Hybrid Coordinate Ocean Model reanalysis from the US Navy	8 km
MERRA	Modern Era Reanalysis for Research and Applications v2	50 km
MODIS	Moderate-imaging Infrared Spectrometer (colour)	4 km
SADW	S.A. Dept of Water Hydrology Service	Gauge
SODA	Simple Ocean Data Assimilation v3 reanalysis	25 km
Wave-watch	Wave Analysis Model hindcast v3 coupled with GFS weather model	50 km

https://doi.org/10.5194/os-2019-55
Preprint. Discussion started: 5 August 2019

Ocean Science
Discussions

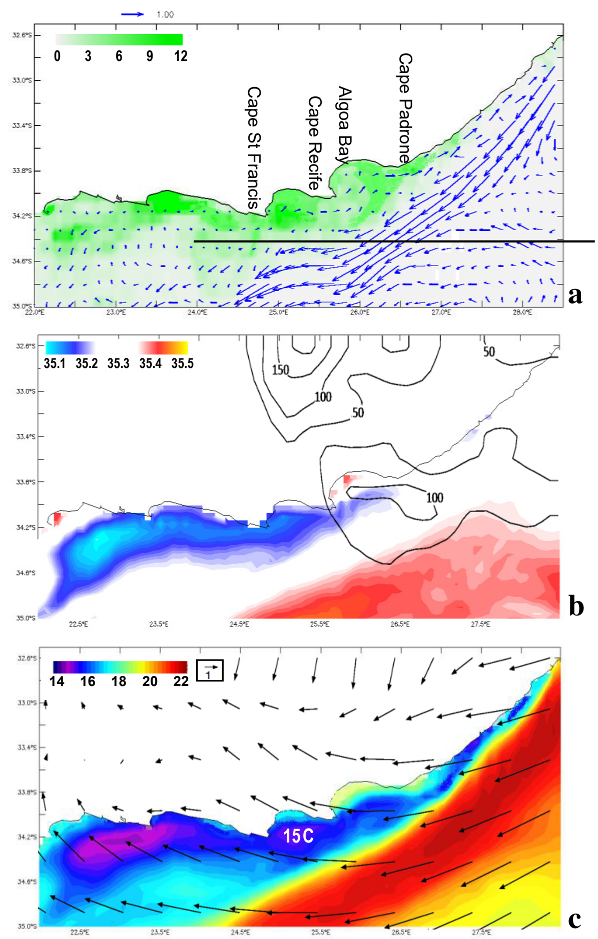

Figure A1 Case study productive event 24 Oct - 8 Nov 2009: (a) MODIS chlorophyll (mg/m^3) and HYCOM currents at 10 m depth (vector), (b) HYCOM salinity at 10 m depth and cumulative CMORPH rainfall > 50 mm (contour), (c) SST map and MERRA2 surface winds (vector). Easterly flow, inshore upwelling and high rainfall characterize this event. Thin west-east line in (a) refers to 34.5S section for Fig A2 below.

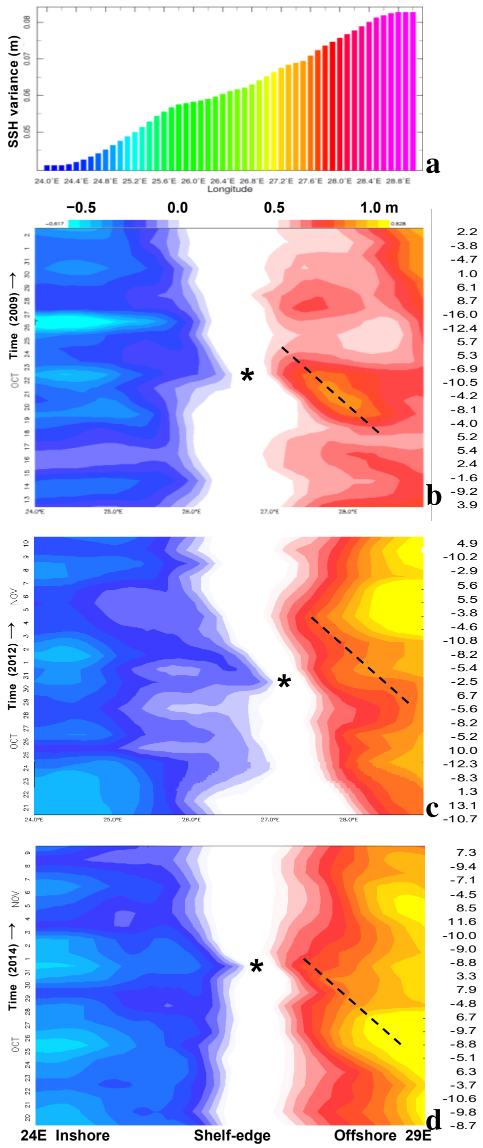

Figure A2 (a) Variance (RMS) of sea surface height anomalies on 34.5S per 0.1° longitude, 2006-2017. Hovmoller plots of HYCOM daily sea surface height on 34.5S over 20 days during three early summer chlorophyll fluorescence events: (b) 2009, (c) 2012, (d) 2014. Asterisk highlights steepest SSH gradient; dashed lines highlight ~0.2 m/s westward movement of anticyclonic warm rings in the offshore zone. Numbers in the right column are index-area daily zonal winds (m/s, -U from east).